Chimica Techno Acta
published by Ural Federal University
eISSN 2411-1414
chimicatechnoacta.ru

ARTICLE
2024, vol. 11(4), No. 202411416
DOI: 10.15826/chimtech.2024.11.4.16

Influence of feedstock composition on the pressure drop buildup in gas oil hydrotreater

Ivan A. Mik *, Oleg P. Klenov, Ivan S. Golubev, Pavel P. Dik, Sergey I. Reshetnikov, Aleksandr S. Noskov

Boreskov Institute of Catalysis SB RAS, Novosibirsk 630090, Russia
* Corresponding author: mikluha.ia@gmail.com

This paper belongs to a Regular Issue.

Abstract

In this work two samples of solid particulates obtained from the intergranular space of the guard beds catalyst of industrial gas oil hydrotreating reactors were investigated. The hydrotreating reactors were operated on feedstock of different composition. One of the samples of solid particulates was obtained during hydrotreating of feedstock containing a large amount of sodium and calcium. The compositions of the samples of solid particulates were determined. Quantitative elemental and structural analyses were carried out. As a result, the formed solid particulates contained a large amount of sodium chloride, sulfate and calcium sulfide. The qualitative calculations show that the pressure drop in the guard bed of five-segment rings with a diameter of 16.0 mm, due to the deposition of solid particulates in the intergranular space, increases by 108% more than the pressure drop during hydrotreating of feedstock not containing calcium and sodium compounds (under the same operating modes of the hydrotreating reactors and operating time). The obtained results on the effect of the feedstock composition on the pressure drop buildup can be used in optimizing the loading of reactors and in other oil refining processes.

Keywords

hydrotreating
guard-bed
particulate trapping
catalyst bed fouling
pressure drop buildup

Received: 03.10.24
Revised: 15.11.24
Accepted: 15.11.24
Available online: 22.11.24

Key findings

- Solid particulates clogging the hydrotreating reactor were studied with different feedstock compositions.
- One of the samples of solid particulates obtained during feedstock hydrotreating contained a large amount of sodium, chlorine and calcium.
- The calculation showed the effect of feedstock composition on the pressure drop buildup in the hydrotreating reactor.
- The results obtained on the effect of feedstock composition on the pressure drop buildup can be used to optimize reactor loading.

© 2024, the Authors. This article is published in open access under the terms and conditions of the Creative Commons Attribution (CC BY) license (http://creativecommons.org/licenses/by/4.0/).

1. Introduction

The pressure drop in catalyst beds is an important production parameter that affects the technical and economic performance of hydrotreating units [1]. Many oil refineries may face the problem of unplanned pressure drop buildup in the hydrotreating reactor. Pressure drop buildup caused by deposits of foulants can lead to hydrotreating process shutdown and the need for complete or partial reload of the hydrotreating catalyst. In industrial practice, to prevent fouling of the main hydrotreating catalyst, beds of guard materials are used, located in the hydrotreating reactor before the main catalyst bed. The guard material pellet size changes from larger to smaller in the direction of the feedstock flow [2]. In this case, the upper beds, which have a high porosity, in the hydroprocessing reactor prevent fouling of the main catalyst bed [2]. Therefore, the operating time of hydroprocessing units can be increased by using a package of varying, in particular, in shape and size, guard-beds [3–8].

The deposition of contaminants in the hydrotreating reactor occurs in the free intergranular volume and on the

surface of the catalysts. The accumulation of microparticulates, coke and resin-containing deposits usually leads to the pressure drop buildup. As a result, the deposits formed in the free volume of the reactor lead to buildup pressure drop and an uneven distribution of the flow. If the deposits settle relatively uniformly in the voids between the catalyst pellets, then the buildup pressure drop in the hydrotreating reactor is a continuous and relatively slow process. In some cases, contaminants and microparticulates accumulate in a relatively narrow area of the guard bed of catalysts, usually between the beds of pellets. [2, 6, 8]. In the latter case, the pressure drop increases more rapidly. As a result, more or less dense carbon-mineral crusts in the hydrotreating reactor can both be destroyed and re-formed. [6, 9–12].

Microparticulates consist of a mixture of particles and agglomerates: corrosion products (iron scale), scale particles from desalination plants (salt, carbonates, etc.) [13], particles of quartz sand (SiO_2, etc.) coming with feedstock [9, 13], catalyst dust and crumbs [14, 15], as well as coke formations. As a rule, the sizes of intergranular microparticulates are different and are in the range from 0.5 to 500 μm.

It is not uncommon when unloading hydrotreating reactors that the microparticulates accumulated in the intergranular space have a red tint. This is due to the fact that the deposits of microparticulates contain a high concentration of iron. During the operation of the hydrotreating unit, erosion of the metal (steel alloys) of which the hydrotreating reactor equipment consists occurs. Therefore, catalytically active particles of iron scale containing coke deposits enter the hydrotreating reactor flow. In the previous work [6] we noted that microparticulates containing iron sulfides (iron scales and their agglomerates) in the voids between the pellets of the hydrotreating reactor may dehydrogenate coke precursors from feedstockstock, resulting in the growth of coke deposits on their surface [6]. Therefore, when microparticulates enter the intergranular space, the growth of coke deposits continues.

In the previous works we investigated the process of accumulation of microparticles in the beds of catalysts of guard beds. This process leads to a decrease in intergranular space, accompanied by an pressure drop buildup [2, 6]. In work [6], aluminum hydroxide particulates were used as model microparticulates, and in work [2] – industrial microparticulates. Due to the complexity of the experiments (creation of industrial hydrotreating conditions for relatively large 16 mm guard bed catalysts), they were carried out at room temperature [2, 6]. In this paper, the effect of the feedstock composition of an industrial hydrotreating unit on the pressure drop buildup in the guard bed catalyst is investigated. The microparticulates of the refinery obtained during the discharge of two industrial gas oil hydrotreating reactors were studied. The difference in the formed microparticulates lies in the mixed composition of the gas oil fractions (sodium and calcium content) fed to the hydrotreating reactors. Probably, the composition of the microparticulates was also affected by the chemical composition of the equipment materials of the industrial hydrotreating units.

In this work, the influence of the feedstock composition on the microparticulates formed in the intergranular space was studied. The compositions of the microparticulate samples were determined. Quantitative elemental and structural analyses were carried out. Based on the data obtained, the pressure drop buildup in the guard bed catalyst for feedstock with different contents sodium and calcium was estimated. In other words, the experiments took place in industrial conditions at an oil refinery (industrial samples). Therefore, there are no analogues of the presented work, since for the first time the data were obtained on how the feedstock composition (sodium and calcium content) affects the pressure drop buildup.

2. Experimental

Two samples of microparticulates in the form of fine powder were obtained during unloading of the catalysts of the guard bed of each of two industrial reactors of gas oil hydrotreatment operating on different feedstocks (feedstocks No. 1 and No. 2). The unloading was carried out after equal operating modes of the hydrotreatment units and operating time. The productivity of both industrial hydrotreatment units (including reactors) was 670 thousand tons of feedstocks per year. Two samples of microparticulates in the form of fine powder were studied by various physicochemical methods listed below.

Scanning electron microscopy. The image was obtained on a JEM-2010 electron microscope (JEOL, Japan) at an accelerating voltage of 200 kV. The samples of microparticulates were fixed on a standard conductive material, which was placed in a holder and introduced into the sample chamber of the electron microscope.

X-ray fluorescence analysis. For X-ray fluorescence analysis (XFA) of all microparticulates samples, the ARL Perform'X (Thermo Scientific) device was used. The tablets were formed using an Atlas Power T25 (Speciac) automatic press, and the samples were weighed on an MV-210-A Gosmetr automatic scale.

Atomic emission spectrometry with inductively coupled plasma (ICP-AES). Quantitative elemental analysis of microparticulates samples was performed by the method of atomic emission spectroscopy with inductively coupled plasma (ICP-AES). Weighing of the samples was performed on Sartorius CP2P balance (Germany). For ICP-AES, the Optima 4300 DV device, Perkin Elmer, was used.

CHNS analysis. Elemental analysis was performed on a EURO EA 3000 automatic CHNS analyzer. The samples were weighed on a Sartorius CP2P balance (Germany). Sample combustion occurred in a vertical reactor in dynamic mode at 1050 °C, in a He flow, with the addition of O_2 (10 ml) at the moment of sample introduction. The resulting N_2, CO_2, H_2O and SO_2 were separated on a column

 DOI: 10.15826/chimtech.2024.11.4.16

with Porapak Q and determined by a thermal conductivity detector (katharometer). The calculation was performed using the Callidus program supplied with the analyzer.

X-ray diffraction analysis (XRD). Transmission diffraction experiments were carried out using Mo Kα radiation (λ=0.7093 Å) on a STOE STADI MP instrument (STOE, Germany) with a MYTHEN2 1K detector (Dectris AG, Switzerland). The measurements were carried out by scanning in the angular range of 2–32° with a step of 0.015° by 2θ. Qualitative X-ray diffraction analysis of the samples was carried out using the ICDD PDF-4+ database. The average size of the coherent scattering region (CSR) of the crystalline phases was determined from the peak broadening data using the Scherrer equation, taking into account the instrumental broadening. The relative content of crystalline phases was estimated based on the full-profile analysis by the Rietveld method.

3. Results and Discussion

Figure 1 shows a high-resolution scanning electron microscopy image of microparticulates in sample No. 1; the image of sample No. 2 does not bring new visual information to the study and is therefore not shown. The micrograph shows the shape of the microparticulates and their characteristic sizes. As a result of the analysis, the size of the microparticles varied from approximately 1 to 80 μm.

Table 1 shows the results of analyses of two types of feedstocks used in industrial hydrotreating reactors. The samples of microparticulates, No. 1 and No. 2, were collected from these industrial reactors. According to the results of the feedstock analysis (Table 1), the fundamental difference between samples No. 1 and No. 2 is that the microparticulates of sample No. 2 were obtained during hydrotreating of the feedstock with a high sodium and calcium content. This feedstock (sample No. 2) can be used in a hydrotreating unit if the process of desalting petroleum feedstock is economically expensive in terms of equipment cost (electrostatic separators, etc.) and the associated operational costs at the refinery.

Tables 2–4 show the results of various independent elemental analyses (X-ray fluorescence analysis, ICP-AES, CHNS, X-ray phase analysis) of micriparticulats samples No. 1 and No. 2.

From the data (Table 2) it is evident that the iron content in sample No. 1 is significantly higher than that in sample No. 2. In turn, sample No. 2 has a high content of chlorine and calcium.

The ICP-AES analysis data (Table 3) confirm the XRF results, namely the percentage of iron and calcium in the samples. In addition, a relatively large amount of sodium (15%) was found in sample No. 2.

The feedstock No. 2 contains a higher amount of calcium (Table 1). Tables 2 and 3 also show that the calcium content of microparticulates sample No. 2 is significantly higher than that of sample No. 1.

The feedstock No. 2 has a sulfur content that is approximately twice as high as that of feedstock No. 1 (Table 1). Table 2 shows that the microparticulates sample also has a higher sulfur content.

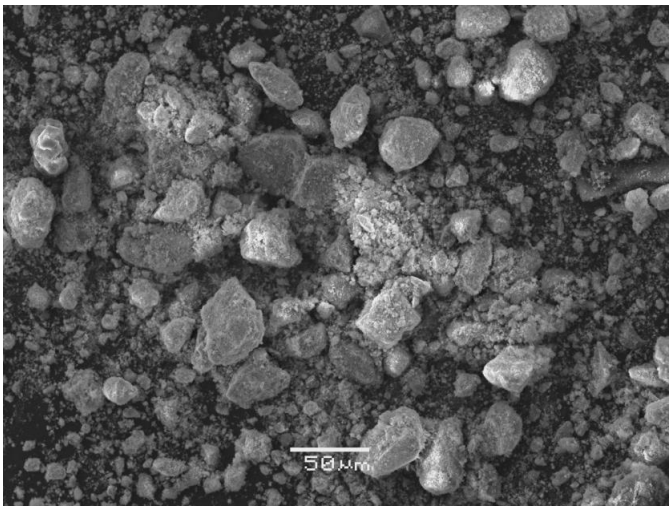

Figure 1 Electron microscopic image of microparticulates No. 1.

Table 1 Analysis of types of feedstocks as a result of the industrial hydrotreating process in the reactor of which microparticulates No. 1 and No. 2 were formed.

Method	Characteristic	Sample No. 1 Feedstock	Sample No.2 Feedstock
ASTM D7213, fractional composition of feedstock, % mass.	b.p.	204	177
	10	275	252
	20	314	295
	30	335	322
	40	356	345
	50	375	376
	60	395	395
	70	425	412
	80	454	445
	90	525	495
	95	550	535
ASTM D4294	S, ppm	1997	1003
	N, ppm	367	356
UOP 407	Fe, ppm	1.3	1.5
	Na, mg/kg	0.02	4.2
	Ca, mg/kg	0.05	2.3

Table 2 X-ray fluorescence analysis of microparticulates samples, % by weight.

Element	Sample No. 1	Sample No. 2
Al	7.1	4.3
Cl	–	19.9
S	23.8	14.6
Ca	0.11	10.9
Ti	–	0.09
Fe	38.1	9.5
Cr	0.60	0.07
Mn	0.81	0.09
Ni	0.99	0.05
Cu	0.1	–

 DOI: 10.15826/chimtech.2024.11.4.16

Table 3 AES-ICP samples of microparticulates, mass fraction, %.

Element	Sample No. 1	Sample No. 2
Al	2.0	0.86
Ca	0.60	10.7
Cr	0.57	<0.04
Cu	0.06	–
Fe	41.6	8.9
K	–	0.50
Mg	0.07	0.43
Mo	0.54	–
Mn	0.36	<0.08
Na	0.17	15.0
Ni	1.8	–

Table 4 CHNS analysis of microparticulates samples, % by weight.

Element	Sample No. 1	Sample No. 2
C	13.1	4.4
H	1.1	0.6
N	0.4	<0.1
S	25.0	9.36

The sodium content of feedstock No. 2 is significantly higher than that of feedstock No. 1 (Table 1). Accordingly, elemental analysis confirms a much higher sodium content in microparticle sample No. 2 (Table 3). From the data in Tables 2 and 3, it can be concluded that sample No. 2, in addition to sulfur and iron, contains a large amount of sodium, chlorine, and calcium. The difference in the percentage content of other elements (Ti, Cr, Mn, Ni, Cu, K, Mg, Mo, Mn) in microparticulates is probably due to the different materials of the industrial installations on which samples No. 1 and No. 2 were obtained, for example, various types of alloy steels used in the equipment of the installations, etc.

Table 4 shows the results of CHNS analysis of the microparticulates samples. Sample No. 1 has a higher carbon content (~13%), which may indicate the presence of coke deposits. This is due to the fact that the feedstock processed in reactor No. 1 contained twice as much sulfur (1997 ppm) compared to reactor No. 2 (1003 ppm), which follows from the data in Table 1. Hydrotreating feedstock with a high sulfur content requires a higher temperature, which contributes to an increase in the rate of formation of carbon deposits (coke formation).

Using X-ray structural analysis, a diffraction pattern of sample No. 1 of microparticulates was obtained (Figure 2).

According to the X-ray phase analysis data, microparticulates contain various crystalline phases of iron sulfide $Fe_{0.91}S$ (PDF No. 00-029-0725, OSR 25 nm), $Fe_{0.985}S$ (PDF No. 04-003-4470, OSR 45 nm), $(Fe,Ni)_9S_8$ (PDF No. 04-002-3675, OSR 34 nm). A narrow reflection at 12.18^0 (Figure 1) by 2Θ indicates the presence of the quartz phase SiO_2 in the sample (PDF No. 00-046-1045, OSR >100 nm).

The diffraction pattern of sample No. 2 is shown in Figure 3.

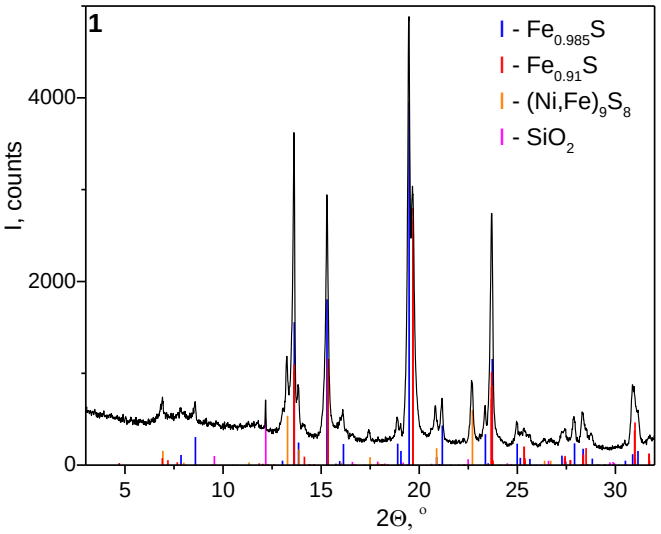

Figure 2 Powder diffraction pattern of sample No. 1.

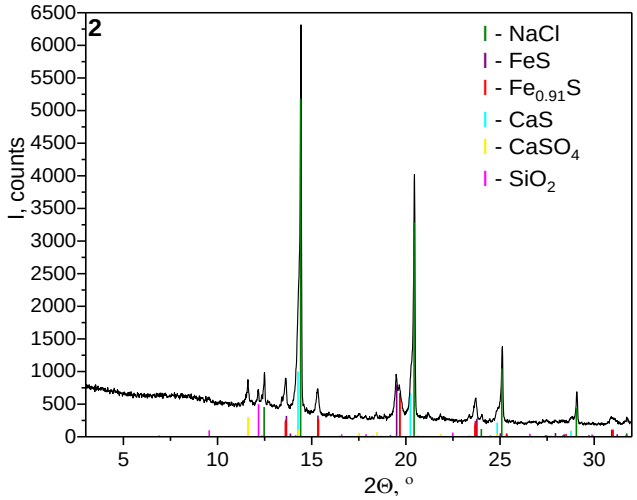

Figure 3 Powder diffraction pattern of sample No.2.

According to the X-ray phase analysis data, microparticulates contain a crystalline phase of sodium chloride NaCl (PDF No. 00-005-0628, RCS > 100 nm), various crystalline phases of iron sulfide $Fe_{0.91}S$ (PDF No. 00-029-0725, RCS > 22 nm), FeS (PDF No. 00-049-1632, RCS > 32 nm), phases of calcium sulfate $CaSO_4$ (PDF No. 00-037-1496, RCS > 38 nm) and calcium sulfide CaS (PDF No. 00-008-0464, RCS > 18 nm), as well as a phase of quartz SiO_2 (PDF No. 00-046-1045, RCS > 100 nm). According to the X-ray phase analysis data, aluminum-containing crystalline phases were not found in the samples. Probably, aluminum is partially included in the composition of iron sulfides or exists in an X-ray amorphous state.

To establish the phase composition of the sediment samples, studies were conducted using the X-ray structural analysis method. Based on the results of this analysis, it was established that the iron in sample No. 1 is in the sulfide form and consists of various structures – $Fe_{0.91}S$, $Fe_{0.985}S$ и $(Fe,Ni)_9S_8$ – approximately 97%. Sample No. 2 consists of sodium chloride – 45%, calcium sulfide – 24%, iron sulfide – 7% of various structures, as well as salts in the form of

 DOI: 10.15826/chimtech.2024.11.4.16

sulfates 9% and 3% quartz sand. Both samples contain particulates of iron sulfides that were formed during the interaction of the iron contained in the feedstock with hydrogen sulfide released during the operation of the hydrotreating reactor. The composition of sample No. 2 indicates that the deposits are formed from sodium, chlorine and calcium salts coming with the processed feedstock, which confirms the chemical elements contained in the feedstock (Table 1).

Due to the high concentration of sodium and calcium in the feedstock, the amount of deposits in sample No. 2 exceeds the amount of iron sulfides. The carbon analysis data (Table 4) also confirm that for sample No. 1 the amount of coke deposits is approximately 3 times greater than in sample No. 2. Calcium and sodium compounds (NaCl, CaS и $CaSO_4$, Table 5) present in high concentration in sample No. 2 are chemically inert to the hydrotreating processes. Therefore, the composition of the feedstock of sample No. 2 will lead to a greater amount of deposits (less free space between catalyst pellets) in the hydrotreating reactor and, accordingly, a greater pressure drop buildup than for the feedstock of sample No. 1, proportional to the volume of deposition of salt compounds.

3.1. The influence estimation of the feedstock composition of the hydrotreating unit on the pressure drop buildup

It can be assumed that the volume of deposits of microparticulates containing iron for two feedstock compositions was approximately the same. By selecting the value of the final porosity of the sample of microparticulates without the content of salt compounds, it is possible to determine the pressure drop buildup for two feedstock compositions (Table 1). Therefore, in order to determine the effect of differences in the feedstock composition on the pressure drop buildup in the pellet bed of five-segment rings (guard bed catalyst), a pressure drop calculation was performed. The following assumptions were made in the calculation:

– deposits of microparticulates are distributed evenly throughout the volume of the catalyst bed;

– particulates of microparticulates in the flow of the hydrotreating unit of two compositions have the same size distributions (electron microscope data);

– microparticulates of the same size have the same collection coefficients by the bed of pellets of five-segment rings;

– the pressure drop buildup occurs due to the growth of the equivalent volume of catalyst pellets and the reduction of the porosity of the bed;

– the growth of intergranular coke deposits occurs at the same rate with different compositions of iron sulfide structures;

– the amount of coke deposits is proportional to the concentration (elemental analysis) of carbon in samples No. 1 and No. 2;

– the density of coke deposits is constant and its value was taken ρ_{coke} = 0.9 g/cm³ [6, 16].

Using the example of a guard bed catalyst in the form of a five-segment ring (Figure 4), the influence of the composition of the feedstock on the pressure drop buildup was shown [2]. The circumscribed circle diameter of the five-segment rings is 16.0 mm, which is a typical size of a guard bed catalyst for modern hydrotreating reactors [6, 17].

Table 6 contains the values of the hydrodynamic parameters taken into account when calculating the pressure drop.

For the given values of hydrodynamic parameters (Table 6), dimensionless hydrodynamic parameters were calculated (Table 7).

An important characteristic that depends on the size and shape of the catalyst particulates is the equivalent diameter (d) [2] of the catalyst pellet, which is taken as the diameter of a sphere having the same volume as the actual catalyst pellet [2, 18]:

$$d = 2\sqrt[3]{\frac{V_p}{4/3 \cdot \pi}}. \quad (1)$$

Table 5 X-ray phase analysis of microparticulates samples, % by weight.

Chemical Compound	Sample No. 1	Sample No. 2
$Fe_{0.91}S$	42	12
$Fe_{0.985}S$	44	–
$(Fe,Ni)_9S_8$	11	–
SiO_2	3	3
NaCl	–	45
FeS	–	7
CaS	–	24
$CaSO_4$	–	9

Table 6 Values of hydrodynamic parameters

Characteristics	Value
Gas superficial velocity, u_{gas}, m/s	0.0981
Oil superficial velocity, u_{liquid}, m/s	0.006
Dynamic viscosity of gas, $v_{gas.}$, Pa·s	$9.8 \cdot 10^{-5}$
Dynamic viscosity of a liquid, v_{liquid}, Pa·s	$1.5 \cdot 10^{-5}$
Gas density, ρ_{gas}, kg/m³	2.78
Density of liquid, ρ_{liquid}, kg/m³	851.1
Mass velocity of gas, G_{gas}, kg/(m² s)	0.27
Mass velocity of liquid, G_{liquid}, kg/(m² s)	5.1

Table 7 Dimensionless parameters

Characteristics	Value
Gas to liquid velocity ratio, u_{gas} / u_{liquid}	16.3
Reynolds number of gas, Re_{gas}	246
Reynolds number of liquid, Re_{liquid}	734

Figure 4 Shape of the pellet of the catalyst guard bed

 DOI: 10.15826/chimtech.2024.11.4.16

For the selected catalyst in the form of a five-segment ring, d is 14 mm.

The loading pressure drop (ΔP) for a two-phase flow through a guard bed catalyst stack can be estimated using Ergun's formula [19, 20]:

$$\frac{\Delta P_i}{\Delta Z} = \frac{150(1-\varepsilon)^2 u_i \nu_i}{\varepsilon^3 d_e^2} + \frac{1.75(1-\varepsilon) u_i^2 \rho_i}{\varepsilon^3 d_e}, \quad (2)$$

where u_i – superficial velocity; ν_i – dynamic viscosity; i – the index denoting the gas or liquid phase; d_e – equivalent diameter of the catalyst; ΔZ – the height of the catalyst bed (in the calculation 0.15 m); ε – the porosity of the pellet bed.

The pressure drops in both the liquid and gas phases can be related using the parameter χ. For values 0.05 < χ < 30 the following equations are used [20]:

$$\chi = \sqrt[2]{\frac{\Delta P_{liquid}}{\Delta P_{gas}}}, \quad (3)$$

$$\log_{10}\left(\frac{\Delta P}{\Delta P_{gas} + \Delta P_{liquid}}\right) = \frac{0.416}{0.666 + (\log_{10}\chi)^2}. \quad (4)$$

Note that in this calculation the pressure drop depends on the equivalent diameter of the pellet and the porosity of the bed and does not depend on the diameter of the reactor. Taking into account the volume of trapped microparticulates, the final (for the clogging bed) porosity of the bed and the equivalent diameter of the five-segment ring (1) were recalculated.

To calculate the volume of deposits when assessing the pressure drop buildup, the following density values were used: $\rho_{FeS} = \rho_{Fe0.91S} = 4800$, $\rho_{microparticulates\ No.1} = 4233$, $\rho_{microparticulates\ No.2} = 2710$ kg/m³.

In the package of guard beds of hydrotreating reactor catalysts, their heights are selected depending on the parameters of the hydrotreating unit (feedstock, mode, etc.). Usually, in industrial practice, the height of the bed of five-segment rings is about 15 cm, which was chosen for this calculation.

The final porosity of the guard bed catalyst with deposits of microparticulates was selected from the values of the pressure drop buildup, according to the Ergun formula (2–4). The value of the pressure drop buildup relative to the initial one was chosen to be 10%, which corresponds to industrial practice. For the selected bed of five-segment rings and pressure drop buildup (10%), the final porosity value will be 0.536 (the calculation result according to the Ergun formula, with the selected parameters, Table 6). That is, the porosity of the bed (relative to the initial) for the composition of feedstock No. 1 (Table 1) will decrease by 0.014 compared to the initial ($\varepsilon_0 = 0.55$). Based on the values of the final porosity for the composition of feedstock No. 1, the volume of microparticulates and other parameters for the composition of feedstock No. 2 were calculated. The calculation was performed on the basis of the following formulas (5–20):

$$N = \frac{V \cdot (1-\varepsilon_0)}{V_p} \quad (5)$$

$$v_1 = V \cdot (\varepsilon_0 - \varepsilon_1) \quad (6)$$

$$m_{1\_C} = \frac{m_1 \cdot m_{1\_C\_\%}}{100} \quad (7)$$

$$m_{1\_SiO_2} = \frac{(m_1 - m_{1\_C}) \cdot m_{1\_SiO_2\_\%}}{100} \quad (8)$$

$$m_{1\_Fe} = m_1 - m_{1\_C} - m_{1\_SiO_2} \quad (9)$$

$$m_{1\text{-}\_Fe} = m_1 \cdot \left(1 - \frac{m_{1\_C\_\%}}{100}\right) \cdot \left(1 - \frac{m_{1\_SiO_2\_\%}}{100}\right) \quad (10)$$

$$v_{1\_Fe} = \frac{v_1 \cdot \rho_{microparticulates\ No.1}}{\rho_{FeS}} \cdot \left(1 - \frac{m_{1\_C\_\%}}{100}\right) \cdot \left(1 - \frac{m_{1\_SiO_2\_\%}}{100}\right) \quad (11)$$

$$v_{2\_Fe} = v_{1\_Fe} \quad (12)$$

$$m_{2\_Fe} = v_{2\_Fe} \cdot \frac{m_{2\_Fe0.91S\_\%} \cdot \rho_{Fe0.91S} + m_{2\_FeS\_\%} \cdot \rho_{FeS}}{m_{2\_Fe0.91S\_\%} + m_{2\_FeS\_\%}} \quad (13)$$

$$m_{2\_SiO_2} = \frac{m_{2\_Fe} \cdot m_{2\_SiO_2\_\%}}{m_{2\_Fe0.91S\_\%} + m_{2\_FeS\_\%}} \quad (14)$$

$$m_{2\_wt\_C} = \frac{100 \cdot (m_{2\_Fe} + m_{2\_SiO_2})}{m_{2\_Fe0.91S\_\%} + m_{2\_FeS\_\%} + m_{2\_SiO_2\_\%}} \quad (15)$$

$$m_{2\_C} = \frac{m_{2\_wt\_C} \cdot m_{2\_C\_\%}}{100 - m_{2\_C\_\%}} \quad (16)$$

$$m_2 = m_{2\_wt\_C} + m_{2\_C} \quad (17)$$

$$v_2 = \frac{m_2}{\rho_{microparticulates\ No.2}} \quad (18)$$

$$\varepsilon_2 = \varepsilon_0 - \frac{v_2}{V} \quad (19)$$

$$d_2 = 2\sqrt[3]{\frac{V \cdot (1-\varepsilon_0) + v_2}{4/3 \cdot \pi \cdot N}} \quad (20)$$

where V – volume of loaded catalyst in the form of five-segment rings, m³; V_p - volume of a five-segment ring pellet, m³; ε – bed porosity; ε_0 – initial porosity of the bed; d_2 – final equivalent diameter of catalyst for feedstock composition No. 2, m; m_i – weight with corresponding indices, kg (data from Table 4 or 5); v_j – volume of deposits in the intergranular space with corresponding indices, m³; ρ_k – density with the corresponding index, kg/m³; $m_{2\_wt\_C}$ – mass of deposits in the intergranular space excluding coke deposits for feedstock composition No. 2, kg, i.e., the indices in formulas (5–20) specify information about the corresponding parameter, for example, indices 1

 DOI: 10.15826/chimtech.2024.11.4.16

and 2 mean the composition of feedstocks No. 1 and No. 2, respectively; index C - coke deposits; index Fe - compounds containing iron (see Table 5); SiO_2 - silicon dioxide; index % - used for mass and means that the parameter specifies the mass percentage in the sample; indices $Fe_{0.91S}$ or FeS - iron sulfides.

Using mathematical relationships (6–11), the volume of compounds containing iron was calculated for the composition of feedstock No. 1 (v_{1_Fe}). Next, from equations (12–18), the volume of "all" microparticulates was calculated for the composition of feedstock No. 2 (v_2). Formulas (7), (8), (10), (14–16) are obtained from mathematical proportions that use the mass concentration data in samples No. 1 and No. 2 (from Table 4 or 5). Formulas (9) and (17) are mass balance equations for the composition of feedstock No. 1 and No. 2. Since all parameters of the industrial hydrotreating process except for the feedstock composition (microparticulates No. 1 and No. 2) were approximately the same, the concentration of iron sulfide compounds in the flow of the two hydrotreating reactors was approximately the same. This means that with equal concentrations of iron sulfides in the reactor flow and the coefficient of microparticle capture by the catalyst bed, the volume of iron-containing deposits for the two reactors (No. 1 and No. 2) will be approximately the same. Therefore, in the calculation v_{1_Fe} is equal to v_{2_Fe} (see formula 12). The proposed calculation was solved mathematically using the GNU Octave software. Some numerical values of the parameters used in the formulas (5–20) are given in Table 8. Table 9 shows the results of the pressure drop calculation for two feedstock compositions of the hydrotreating unit.

Therefore, the difference in the pressure drop buildup for two microparticulates compositions depends on the percentage content of sodium chloride, calcium sulfide - hardness salts in the form of sulfates and coke deposits in sample No. 2. The assessment assumes equal volumes of iron sulfides in the hydrotreating reactor flow (see iron content in Table 1) and, taking into account the significant volume of salt deposits in sample No. 2, the bed porosity of sample No. 2 decreased to 0.445 (Table 9). Due to this, if, with the selected calculation parameters (Table 6), the feedstock fed to the reactor "does not contain" salts (feedstock of sample No. 1, Table 1), then the pressure drop in the bed of five-segment rings will increase from the initial value of 13.6 Pa to 15.0 Pa (by 10%).

If the sodium and calcium content in the hydrotreating reactor feedstock is 4.2 and 2.4 mg/kg (sample feedstock No. 2), respectively, then the pressure drop relative to the initial value (13.6 Pa) will increase to 29.8 Pa (by 118%). That is, the concentration of sodium and calcium (4.2 and 2.4 mg/kg, respectively) in the feedstock significantly increases the amount of deposits in the intergranular space, which, in comparison with feedstock without salt compounds (sample feedstock No. 1), increases the pressure drop by 108%.

Table 8 Values of parameters used in the process of calculating the final porosity and equivalent diameter of the catalyst

Characteristics	Sample No. 1 Feedstock	Sample No. 2 Feedstock
Volume of loaded catalyst (V), m^3	0.6232	
Initial porosity of the bed (ε_0)	0.55	
Volume of a five-segment ring pellet (V_p), m^3	$1.43 \cdot 10^{-6}$	
The number of pellets of loaded catalyst with a bed height of 15 cm (N), pcs.	196350	
Volume of iron-containing deposits (v_{j_Fe}), m^3	0.0067	
Volume of "all" microparticulates (v_j), m^3	0.0087	0.0652

Table 9 Estimation of pressure drop buildup in hydrotreating reactors depending on feedstock composition

Characteristics		Sample No. 1 Feedstock	Sample No. 2 Feedstock
Concentration of Na and Ca in feedstock		Low	High
Clean catalyst bed	Pressure drop (ΔP), Pa	13.6	
	Bed porosity (ε_j)	0.536	0.445
Clogged catalyst bed	Equivalent diameter of catalyst (d), mm	14.1	15.0
	Pressure drop (ΔP), Pa	15.0	29.8

4. Limitations

In this study, some limitations were introduced in the calculation of the pressure drop. The calculation assumed that deposits of micropaticulates are distributed evenly throughout the volume of the catalyst bed. This limitation is due to the fact that the studied samples were taken from industrial reactors where it was possible to obtain only an average amount of deposits in the bed. This is also why the pressure drop calculations in the study are estimates. Future studies are planned to conduct laboratory experiments with the distribution of deposits by the height of the catalyst bed.

5. Conclusions

In this work two samples of microparticulates obtained from the intergranular space of the guard bed catalyst of industrial gas oil hydrotreating reactors operating on different feedstocks were investigated. One of the samples of microparticulates was obtained during hydrotreating of feedstock containing a large amount of sodium and calcium (4.2 and 2.4 mg/kg, respectively). As a result, the formed microparticulates contained a large amount of sodium chloride, sulfate and calcium sulfide (NaCl, CaS and $CaSO_4$). The

 DOI: 10.15826/chimtech.2024.11.4.16

qualitative calculations show that the pressure drop in the guard bed of five-segment rings (diameter 16.0 mm), due to the deposition of microparticulates in the intergranular space (composition No. 2), increases by 108% more than the pressure drop during hydrotreating of feedstock not containing calcium and sodium compounds (composition No. 1) under the same operating modes of hydrotreating reactors and operating time.

The obtained results on the influence of the composition of the feedstock on the hydraulic resistance buildup can be used in optimizing the loading of reactors and in other oil refining processes.

• Supplementary materials

No supplementary materials are available.

• Funding

This work was supported by the Russian Science Foundation (project no. 23-19-00214).

• Acknowledgments

None.

• Author contributions

Conceptualization: I.A.M., S.I.R.
Data curation: I.A.M., S.I.R., K.O.P., P.P.D., I.S.G.
Validation and formal analysis, I.A.M., S.I.R., K.O.P., P.P.D., I.S.G.
Writing: I.A.M., S.I.R., A.S.N.
Investigation: I.A.M.
Supervision and project administration, I.A.M., A.S.N., S.I.R.

• Conflict of interest

The authors declare no conflict of interest.

• Additional information

Author IDs:
Ivan A. Mik, Scopus ID 55375424900;
Oleg P. Klenov, Scopus ID 6506012360;
Ivan S. Golubev, Scopus ID 57204059505;
Pavel P. Dik, Scopus ID 36501421600;
Sergey I. Reshetnikov, Scopus ID 7004434230;
Aleksandr S. Noskov Scopus ID 7005685096.

Website:
Boreskov Institute of Catalysis SB RAS, https://en.catalysis.ru/.

References

1. Budukva SV, et al. Deactivation of hydrotreating catalysts (A review). Katal v promyshlennosti. 2022;22(3):38–65. doi:10.18412/1816-0387-2022-3-38-65
2. Mik IA, et al. Guard of hydrotreating catalysts of oil fractions from solid particulates: experimental studies and calculation. Katal v promyshlennosti. 2023;23(6):70–79. doi:10.18412/1816-0387-2023-6-70-79
3. Hamidipour M., Larachi F., Ring Z. Monitoring Filtration in Trickle Beds Using Electrical Capacitance Tomography. Ind Eng Chem Res. 2009;48(3):1140–1153. doi:10.1021/ie800810t
4. Robinson PR, Dolbear GE. Hydrotreating and Hydrocracking: Fundamentals. Practical Advances in Petroleum Processing. New York, NY: Springer New York. 177–218. doi:10.1007/978-0-387-25789-1_7
5. Dalai A.K. et al. Deposition of fine particles during hydrotreating of oil sands bitumen-derived heavy gas oil in a packed bed reactor: Impact of process parameters and surface charge. Ind Eng Chem Res. 2021;60(43):15464–15471. doi:10.1021/acs.iecr.1c03000
6. Mik IA, et al. Optimization of grading guard systems for trapping of particulates to prevent pressure drop buildup in gas oil hydrotreater. Fuel. 2021;285. doi:10.1016/j.fuel.2020.119149
7. Nadeina KA, et al. Influence of alumina precursor on silicon capacity of NiMo/γ-Al_2O_3 guard bed catalysts for gas oil hydrotreating. Catal Today Elsevier BV. 2019;353:53–62. doi:10.1016/j.cattod.2019.10.028
8. Nadeina KA, et al. Guard bed catalysts for silicon removal during hydrotreating of middle distillates. Catal Today. 2019;329:53–62. doi:10.1016/j.cattod.2018.11.075
9. Edouard D, Iliuta I, Larachi F. Role of gas phase in the deposition dynamics of fine particles in trickle-bed reactors. Chem. Eng. Sci. 2006; 61(12):3875-3884. doi:10.1016/j.ces.2006.01.031
10. Rana R, et al. Deposition of fine particles of gas oil on hydrotreating catalyst: Impact of process parameters and filtration trends. Fuel Process Technol. 2018;171:223–231. doi:10.1016/j.fuproc.2017.09.019
11. Rana R, et al. The Impact of Process Parameters on the Deposition of Fines Present in Bitumen-Derived Gas Oil on Hydrotreating Catalyst. Energy and Fuels. Am Chem Soc. 2017;31(6):5969–5981. doi: 10.1021/acs.energyfuels.7b00554
12. Moyse BM. Raschig ring hds catalysts reduce pressure drop. Oil Gas J. 1984;82(53):164–166.
13. Polischuk C, et al. Impact of Fine Solids on Hydrotreating of Bitumen-Derived Gas Oil. Ind Eng Chem Res. 2023;62(2):936–948. doi:10.1021/acs.iecr.2c04241
14. Speight JG. Fouling in refineries. Fouling in Refineries. 2015):1–538. doi:10.1016/C2013-0-19044-7
15. J. Ancheyta. Deactivation of Heavy Oil Hydroprocessing Catalysts: Fundamentals and Modeling. 2016:336.
16. Wang W, et al. Different Mechanisms of Coke Precursor Formation in Thermal Conversion and Deep Hydroprocessing of Vacuum Residue. Energy Fuels. 2016. doi:10.1021/acs.energyfuels.6b01488
17. Ancheyta J. Modeling and Simulation of Catalytic Reactors for Petroleum Refining. Modeling and Simulation of Catalytic Reactors for Petroleum Refining. 2011.
18. Ancheyta J, Muñoz JAD, Macías MJ. Experimental and theoretical determination of the particle size of hydrotreating catalysts of different shapes. Catal Today Elsevier, 2005;109(1–4):120–127. doi: 10.1016/j.cattod.2005.08.009
19. Felder RM. Catalytic reactor design, by M. Orhan Tarhan. McGraw-Hill, 1983. AIChE Journal. 1984;30(1):173–173.
20. Macías MJ, Ancheyta J. Simulation of an isothermal hydrodesulfurization small reactor with different catalyst particle shapes. Catal. Today. 2004;98(1):243–252. doi:10.1016/j.cattod.2004.07.038

 DOI: 10.15826/chimtech.2024.11.4.16